

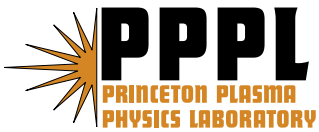
---

# Princeton Plasma Physics Laboratory

---

PPPL-

PPPL-



Prepared for the U.S. Department of Energy under Contract DE-AC02-09CH11466.

# Princeton Plasma Physics Laboratory

## Report Disclaimers

---

### Full Legal Disclaimer

This report was prepared as an account of work sponsored by an agency of the United States Government. Neither the United States Government nor any agency thereof, nor any of their employees, nor any of their contractors, subcontractors or their employees, makes any warranty, express or implied, or assumes any legal liability or responsibility for the accuracy, completeness, or any third party's use or the results of such use of any information, apparatus, product, or process disclosed, or represents that its use would not infringe privately owned rights. Reference herein to any specific commercial product, process, or service by trade name, trademark, manufacturer, or otherwise, does not necessarily constitute or imply its endorsement, recommendation, or favoring by the United States Government or any agency thereof or its contractors or subcontractors. The views and opinions of authors expressed herein do not necessarily state or reflect those of the United States Government or any agency thereof.

### Trademark Disclaimer

Reference herein to any specific commercial product, process, or service by trade name, trademark, manufacturer, or otherwise, does not necessarily constitute or imply its endorsement, recommendation, or favoring by the United States Government or any agency thereof or its contractors or subcontractors.

---

## PPPL Report Availability

### Princeton Plasma Physics Laboratory:

<http://www.pppl.gov/techreports.cfm>

### Office of Scientific and Technical Information (OSTI):

<http://www.osti.gov/bridge>

---

### Related Links:

[U.S. Department of Energy](#)

[Office of Scientific and Technical Information](#)

[Fusion Links](#)

# Refractive and relativistic effects on ITER low field side reflectometer design<sup>a)</sup>

G. Wang,<sup>1,b)</sup> T.L. Rhodes,<sup>1</sup> W.A. Peebles,<sup>1</sup> R.W. Harvey,<sup>2</sup> and R.V. Budny<sup>3</sup>

<sup>1</sup>University of California, Los Angeles, California 90095, USA

<sup>2</sup>CompX, Del Mar, CA 92014, USA

<sup>3</sup>Princeton Plasma Physics Laboratory, Princeton, New Jersey 08543, USA

(Presented XXXXX; received XXXXX; accepted XXXXX; published online XXXXX)

(Dates appearing here are provided by the Editorial Office)

The ITER low field side reflectometer faces some unique design challenges, among which are included the effect of relativistic electron temperatures and refraction of probing waves. This paper utilizes GENRAY, a 3-D ray tracing code, to investigate these effects. Using a simulated ITER operating scenario, characteristics of the reflected RF waves returning to the launch plane are quantified as a function of a range of design parameters, including antenna height, antenna size, and antenna radial position. Results for edge/SOL measurement with both O- and X-modes using proposed antennas are reported.

## I. INTRODUCTION

Reflectometry is a proven diagnostic employing an FM-CW radar technique for electron density profiles on a wide range of fusion plasmas, e.g. DIII-D [1,2], NSTX [3], ASDEX-U [4], and Tore Supra [5], etc. It launches a probing microwave/millimeter wave into the plasma, perpendicular to the magnetic field, and measures the phase delay due to the plasma as the wave is reflected back from either the O- or X-mode cutoff point in the plasma. The electron density profile can then be inferred from the frequency dependence of the phase, which can be obtained by sweeping the frequency of the probing wave.

Reflectometry is well suited to the harsh fusion environment in ITER and a low field side (LFS) reflectometer including both O- and X-mode waves has been planned [6] for scrape off layer (SOL), edge, and core measurements. However, in ITER, reflectometry faces some unique design challenges. First, due to high electron temperature in ITER plasmas, the relativistic electron effect [6], which strongly affects both cutoff position and beam propagation, needs to be assessed. Second, the refractive effect of the plasma on the probing wave needs to be assessed for effective receiving, due to the present requirement that multiple fixed waveguide antennas measure a variety of plasma conditions.

This paper utilizes GENRAY to investigate refractive and relativistic effects on ITER LFS reflectometer design. GENRAY [7] is a general 3-D ray tracing code for the calculation of electromagnetic wave propagation and absorption in the geometrical optics approximation using generalized magnetic equilibrium and density and temperature profiles. It is applicable to ITER LFS reflectometer study [8] due to a much larger scale of plasma properties than the microwave/millimeter wave wavelength. In previous reflectometer ray tracing studies, beam drift and distortion were found, and they were found to be correlated with local magnetic field at cutoffs [8,9]. Using a simulated ITER H-mode scenario 2 [10], characteristics of the reflected RF waves returning to the launch plane are quantified as

a function of three design parameters: antenna height, antenna size, and antenna radial position. Results for edge/SOL measurement with both O- and X-modes using proposed antennas are reported.

## II. DESCRIPTION OF THE ANALYSIS METHOD

GENRAY implements several different dispersion function models for different plasma applications, including e.g. cold plasma approximation, and relativistic electrons. In this study, for relativistic electron plasma, GENAY uses the approximation of the relativistic dielectric tensor and the dispersion relation proposed by Mazzucato [11].

The front-end design of the LFS reflectometer in ITER currently employs low-loss corrugated waveguide launching a Gaussian-like HE<sub>11</sub> wave mode. For a Gaussian beam, its width is defined as the radius at which the power drops to  $1/e^2$  of the axial value, can be written as  $w(x) = w_0 \sqrt{1 + (x/x_R)^2}$

where  $x_R = \pi w_0^2 / \lambda$ ,  $\lambda$  is wavelength,  $x$  is the distance along the beam from the beam waist where  $w$  is minimal ( $=w_0$ ). Shown in Fig. 1(a) is Gaussian beam width (the 2 thinner solid curves) in free space for a 161 GHz wave launched from  $d=3$  cm diameter waveguide antenna located at  $R=8.4978$  m where the wall is. The half-width of the waist is assumed  $w_0=0.96$  cm ( $=0.32*d$ ) for optimal coupling of launch and receive of the HE<sub>11</sub> mode with a corrugated waveguide antenna [12]. The LCFS is shown as the thicker vertical line for ITER H-mode Scenario 2 plasma configuration. The antenna height is 15 cm above the magnetic axis for this scenario. The lines that are tangent to the Gaussian beam width curves when intersecting the LCFS form a 3-D incident beam cone, as shown by the shaded area in the poloidal cross-section in Fig. 1(a).

Fig. 1(b) shows density and temperature profiles for the simulated ITER H-mode scenario 2. Radial profiles of O-mode and right-hand X-mode cutoff frequencies for cold plasma

<sup>a)</sup>Contributed paper published as part of the Proceedings of the 18th Topical Conference on High-Temperature Plasma Diagnostics, Wildwood, New Jersey, May, 2010.

<sup>b)</sup>Author to whom correspondence should be addressed. Electronic mail: wang@fusion.gat.com.

assumption (dashed curves) and relativistic electrons (solid curves) at magnetic axis height are plotted in Fig. 1(c). It can be clearly seen that both O- and X-mode cutoff frequencies downshift due to relativistic electrons. Relativistic electrons also broaden electron cyclotron (EC) resonant absorption region and may also cause cutoff profiles to be hollow [6], which could potentially affect core plasma access by LFS reflectometer, but this is outside the scope of this paper.

In order to quantify the receive beam spot (footprint) at the launch antenna plane (perpendicular to the launch beam path in the vacuum), 8 incident rays which are uniformly distributed across the 3 dB cone surface are chosen for GENRAY calculation. The returned rays intersect with the antenna plane, and the 8 intersecting points are obtained and fitted with a closed curve to represent the beam spot at the antenna plane.

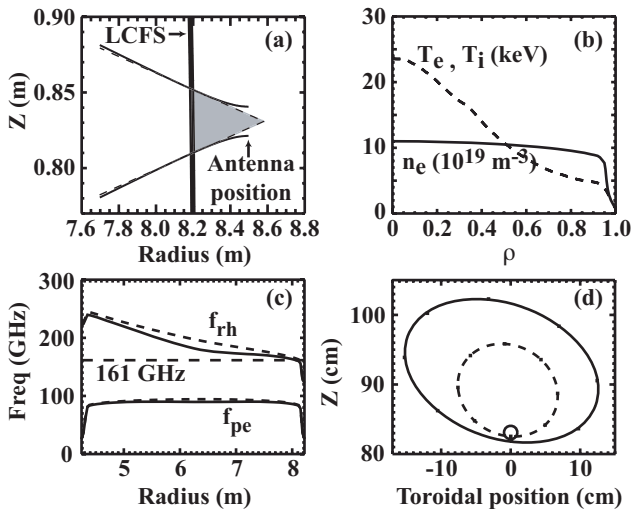


Figure 1 (a) Gaussian beam width (2 thinner solid curves) in free space for 161 GHz launched from 3 cm diameter waveguide antenna. The lines that are tangent to the Gaussian beam when intersecting the LCFS form a 3-D incident beam cone, as shown by the shaded area in the poloidal cross-section. (b) Radial profiles of density, electron and ion temperatures for ITER H-mode Scenario 2, (c) Radial profiles of O-mode and right-hand X-mode cutoff frequencies for cold plasma assumption (dashed curves) and relativistic electrons (solid curves) at magnetic axis height. (d) Launch (small circle) and return (2 larger ovals) beam footprints at the launch plane viewing toward plasma from LFS for cold (dashed curve) and relativistic (solid curve) plasma cases in (c) with 161 GHz, X-mode. The small circle represent the launch beam spot, small squares are the intersecting points of returned rays and the launch antenna plane, and the 2 larger curves are best fit to these points using ellipses.

Fig. 1(d) illustrates the difference of the returned beam spot at the antenna plane for cold plasma assumption (dashed oval) and relativistic electrons (solid oval) with 161 GHz X-mode launch. The curves are best fits to the 8 ray points returned at the antenna plane using ellipses. It can be noticed that both vertical and toroidal drift and distortion can be observed in both cases. Changes in cutoff shape and location due to relativistic effects (shown in Fig. 1(c)) result in large change to beam.

### III. EFFECTS OF LAUNCH ANTENNA HEIGHT, SIZE, AND RADIAL POSITION

In this paper, the front end of the LFS reflectometer design is limited to the selection of launch antenna height, size (i.e. waveguide diameter), and radial position. The fourth free parameter, launch angle is fixed (horizontal) in the current ITER design. To address different plasma heights a vertical array of antennas is currently envisaged. This section will use GENRAY to gain some insight into how the three parameters affect the return signal. The same plasma and 161 GHz X-mode probing wave as in Fig. 1 are used. Figure 2 compared the return beam spot at the antenna plane with different launch antenna heights (Fig. 2(a)), antenna sizes (Fig. 2(b)), and radial positions (Fig. 2(c)) while keeping other parameters the same.

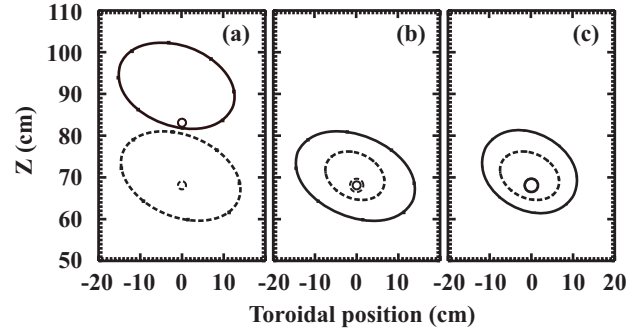


Figure 2 Launch and return beam spots at the antenna plane viewing toward plasma from LFS for the ITER H-mode Scenario 2 plasma with 161 GHz, X-mode incident wave: (a) antenna height is 83 cm (solid curves) versus 68 cm (dashed curves) with the same antenna diameters and radii, (b) antenna diameter is 3 cm (solid curves) versus 5 cm (dashed curves) with the same antenna heights and radii, (c) antenna radius is 8.7978 m (solid curves) versus 8.4978 m (dashed curves) with the same antenna heights and diameters.

In Fig. 2(a), as launch antenna is at vertical height  $z=68$  cm (The magnetic axis for this plasma is at  $z=68.1$  cm), the returned beam is basically symmetric around the launch antenna. When the launch antenna was raised 15 cm higher, the returned beam upshifted  $\sim 10$  cm relative to the launch. This vertical shift has been observed previously [9] and has led to an important understanding that ITER LFS reflectometer should have multiple vertically arranged antennas [13,14].

Fig. 2(b) demonstrates that smaller antenna size results in more diverged return beam. This is because a Gaussian beam has larger divergence at smaller beam waist, where divergence angle is given by  $\theta \approx \lambda/\pi w_0$ . For bi-static antenna configuration, a smaller antenna size is potentially useful as it spreads the return beam over a larger area; but too much divergence raises the question of receive signal level tradeoff. In addition, since  $\theta$  has a wavelength dependence, the whole frequency range needs to be examined (next Section). Fig. 2(c) indicates locating the antenna farther away from the plasma increases the size of the returned beam. This is especially important and useful in order to couple to other nearby antennas. This will be examined in more detail in the next Section.

### IV. RESULTS FOR EDGE/SOL MEASUREMENT USING PROPOSED ANTENNAS

Within the existing available port space for ITER LFS reflectometer, two vertical arrays of antennas are currently being proposed for edge/SOL access using O- and X-mode waves

respectively. Figs. 3(a)-(c) show the 5 O-mode antennas with a diameter of 7.5 cm, separation distance of 10 cm with a design frequency range of 18-60 GHz, and Figs. 3(d)-(f) show the 5 X-mode antennas with a diameter of 3 cm, separation distance of 9 cm with a design frequency range of 50-170 GHz. Note the radial location of the antennas is 8.7978 m, i.e. it is set back 30 cm from the wall than originally planned [6]. This arrangement provides a reasonably big antenna size for a less divergent beam for the sweeping frequency range to ensure enough returned power.

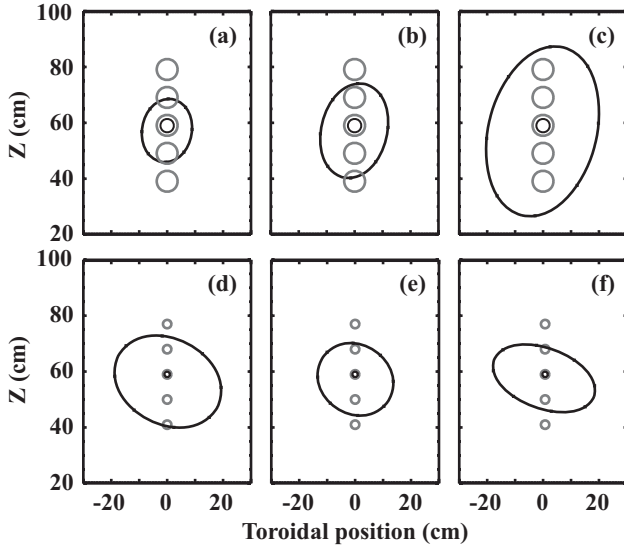


Figure 3 Launch (small, dark, solid circles) and return (dark, solid ellipses) beam spots at the antenna plane viewing toward plasma from LFS for ITER H-mode Scenario 2 with O-mode (figures (a)-(c), antenna diameters equal 7.5 cm, and  $R=8.7978$  m) and X-mode (figures (d)-(f), antenna diameters equal 3 cm, and  $R=8.7978$  m) for edge measurement using proposed antenna arrays (gray circles). Wave frequencies are: (a) 60 GHz, (b) 41.3 GHz, (c) 21 GHz, (d) 160.8 GHz, (e) 131 GHz, and (f) 122 GHz.

Using the same ITER plasma scenario as in Figures 1-2, launch and return beam footprints at the antenna plane are shown in Figure 3 for 3 cutoff locations in the plasma:  $\rho \sim 0.9$  (at the top of H-mode edge pedestal, Fig. 3(a) and (d)),  $\rho \sim 0.98$  (Fig. 3(b) and (e)), and SOL (21 GHz in Fig. 3(c) and 122 GHz in Fig. 3(f)). Currently GENRAY uses vacuum ray tracing in the SOL. Therefore the return beam footprint from reflection in the SOL is not accurately calculated. As a first approximation to the correct calculation, the density profile is shifted radially inward by 20 cm then placing the SOL density inside the LCFS. For the GENRAY calculation for SOL cases (Figs. 3(c) and 3(f)), the density profile is assumed exponentially decreasing with a decay length of 10 cm. It is noted that this is not a correct treatment of magnetic structure in the SOL but does give a qualitative picture of the returned beam. Future work will correctly address this issue. The calculations do indicate that the returned beam footprint has adequate size to couple to a second antenna (Figs. 3(c) and 3(f)).

It can be seen in Fig. 3 that the return beam overlays with at least one receive antenna. This is the minimum requirement for successful operation. Other requirements include sufficient return signal-to-noise ratio, minimal phase errors due to angle of coupling, etc. which are the subjects of future studies.

## V. CONCLUSION

In summary, GENRAY, a 3-D ray tracing code, has been utilized to investigate refractive and relativistic effects for ITER LFS density profile reflectometer antenna design. Using ITER H-mode scenario 2 plasma, characteristics of the reflected RF waves returning to the launch plane are quantified as a function of a range of design parameters, including antenna height, antenna size, and radial position. With the existing available port space for ITER LFS reflectometer, the two vertical arrays of antennas currently proposed for edge/SOL access using O- and X-mode waves respectively are shown to have adequate return signal patterns. Studies such as these are the first step in a dedicated design program. Future work includes laboratory validation and optimization and full wave calculation.

## ACKNOWLEDGEMENTS

This work is supported by USDOE Grants DE-FG02-08ER54984 and DE-FG02-04ER54744.

- <sup>1</sup>G. Wang, E. J. Doyle, W. A. Peebles, L. Zeng, T. L. Rhodes, S. Kubota, X. Nguyen, and N. A. Crocker, *Rev. Sci. Instrum.* **75**, 3800 (2004).
- <sup>2</sup>L. Zeng, G. Wang, E.J. Doyle, T.L. Rhodes, W.A. Peebles, and Q. Peng, *Nucl. Fusion* **46**, S677 (2006).
- <sup>3</sup>S. Kubota, X. V. Nguyen, W. A. Peebles, L. Zeng, E. J. Doyle, and A. L. Roquemore, *Rev. Sci. Instrum.* **72**, 348 (2001).
- <sup>4</sup>P. Varela, M.E. Manso, A. Silva, the CFN Team and the ASDEX Upgrade Team, *Nucl. Fusion* **46**, S693 (2006).
- <sup>5</sup>R. Sabot, A. Sirinelli, J.-M. Chareau, and J.-C. Giacalone, *Nucl. Fusion* **46**, S685 (2006).
- <sup>6</sup>G. Vayakis, C.I. Walker, F. Clairet, R. Sabot, V. Tribaldos, T. Estrada, E. Blanco, J. S'anchez, G.G. Denisov, V.I. Belousov, F. Da Silva, P. Varela, M.E. Manso, L. Cupido, J. Dias, N. Valverde, V.A. Vershkov, D.A. Shelukhin, S.V. Soldatov, A.O. Urazbaev, E. Yu Frolov, and S. Heurax, *Nucl. Fusion* **46**, S836 (2006).
- <sup>7</sup>A.P. Smirnov, R.W. Harvey, and K. Kupfer, *Bull Am. Phys. Soc.* **39** 1626 (1994).
- <sup>8</sup>P.-A. Gourdain and W.A. Peebles, *Rev. Sci. Instrum.* **79**, 10F102 (2008).
- <sup>9</sup>P.-A. Gourdain and W.A. Peebles, *Plasma Phys. Control. Fusion* **50**, 025004 (2008).
- <sup>10</sup>H. Weisen, Proceedings of the 21st IAEA Fusion Energy Conference, Chengdu, China (unpublished), p. EX/8-4.
- <sup>11</sup>E. Mazzucato, I. Fidone, G. Granata, *Phys. Fluids* **30**, 3745 (1987).
- <sup>12</sup>P.F. Goldsmith, Proceedings of the IEEE **80**, 1279 (1992).
- <sup>13</sup>W.A. Peebles, talk at the 12<sup>th</sup> meeting of ITPA Topical Group on Diagnostics, Princeton, NJ, March 26-30, 2007.
- <sup>14</sup>G.J. Kramer, R. Nazikian, E.J. Valeo, R.V. Budny, C. Kessel and D. Johnson, *Nucl. Fusion* **46**, S846 (2006).

The Princeton Plasma Physics Laboratory is operated  
by Princeton University under contract  
with the U.S. Department of Energy.

Information Services  
Princeton Plasma Physics Laboratory  
P.O. Box 451  
Princeton, NJ 08543

Phone: 609-243-2245  
Fax: 609-243-2751  
e-mail: [pppl\\_info@pppl.gov](mailto:pppl_info@pppl.gov)  
Internet Address: <http://www.pppl.gov>